THE MUON INJECTION SIMULATION STUDY FOR THE MUON g-2 EXPERIMENT AT FERMILAB*

S. Kim† and D. Rubin, Cornell University, Ithaca, NY, USA
D. Stratakis, Fermi National Accelerator Laboratory, Batavia, IL, USA
N. S. Froemming, University of Washington, Seattle, WA, USA

Abstract

The new experiment, under construction at Fermilab, to measure the muon magnetic moment anomaly, aims to reduce measurement uncertainty by a factor of four to 140 ppb. The required statistics depend on efficient production and delivery of the highly polarized muon beams from production target into the g-2 storage ring at the design "magic"-momentum of 3.094 GeV/c, with minimal pion and proton contamination. We have developed the simulation tools for the muon transport based on G4Beamline and BMAD, from the target station, through the pion decay line and delivery ring and into the storage ring, ending with detection of decay positrons. These simulation tools are being used for the optimization of the various beam line guide field parameters related to the muon capture efficiency, and the evaluation of systematic measurement uncertainties. We describe the details of the model and some key findings of the study.

INTRODUCTION

The Muon g-2 Experiment, at Fermilab [1], will measure the muon anomalous magnetic moment, α_μ to unprecedented precision: 0.14 parts per million. This four-fold improvement in experimental precision compared to Brookhaven's experiment [2], could establish beyond doubt a signal for new physics if the central value of the measurement remains unchanged. To perform the experiment, a polarized beam of positive muons is injected into a storage ring with a uniform magnetic field in the vertical direction. Since the positron direction from the weak muon decay is correlated with the spin of the muon, the precession frequency is measured by counting the rate of positrons above an energy threshold versus time. The g-2 value is then proportional to the precession frequency divided by the magnetic field of the storage ring.

Achieving the targeted precision requires optimum transmission of polarized muons within the g-2 storage ring acceptance. The goal of this paper is to develop a simulation model for the Fermilab g-2 experiment. While emphasis in our previous work [3] was given to the beamlines upstream to the storage ring, here we detail our injection to the storage ring scheme as well as evaluate the performance of the ring after multi-turn operation.

* Supported by DOE DE-SC0008037.
† sk2528@cornell.edu

MUON CAMPUS BEAMLINE

Protons with 8 GeV kinetic energy are transported via the M1 beamline to a Inconel target at AP0. Within a 1.33 s cycle length, 16 pulses with 10^{12} protons and 120 ns full length for each, are arriving at the target. Secondary beam from the target will be collected using a lithium lens, and positively-charged particles with a momentum of 3.1 GeV/c (± 10%) will be selected using a bending magnet. Secondary beam leaving the Target Station will travel through the M2 and M3 lines which are designed to capture as many muons with momentum 3.094 GeV/c from pion decay as possible. The beam will then be injected into the Delivery Ring (DR). After several revolutions around the DR, essentially all of the pions will have decayed into muons, and the muons will have separated in time from the heavier protons. A kicker will then be used to abort the protons, and the muon beam will be extracted into the new M4 line, and finally into the new M5 beamline which leads to the (g-2) storage ring (Fig. 1). Note that the M3 line, DR, and M4 line are also designed to be used for 8 GeV proton transport by the Mu2e experiment.

Figure 1: Layout of the Fermilab Muon Campus.

Detailed numerical simulations [3] indicate that at the end of M5, the number of muons per proton on target (POT) within the acceptance $\Delta p/p = \pm 0.5\%$ is $\approx 2.0 \times 10^{-7}$. The beam is centered at 3.091 GeV/c with a spread $\Delta p/p = 1.2\%$ and is 96% polarized.

MUON BEAM INJECTION INTO THE STORAGE RING

The M5 beamline leads the muon beam to the entrance of the muon storage ring. The storage ring is a dipole magnet which provides the 1.451 T, uniform magnetic field (B_0) over the muon storage region. The radius of the storage ring is 7.112 m (R_0) by the center position of the

storage region whose cross section has a radius of 45 mm. The outermost layer of the ring is the iron yoke and between the magnet poles where the dipole field is applied and the inner wall of the iron yoke, there is a 39 cm gap. The magnetic field is zero at the iron surface and it rises to 1.451 T across this gap. Therefore, when the muon beam comes into the ring, it experiences this fringe field from the dipole magnetic field and the path of the incoming beam can be deviated from the ideal trajectory. The superconducting magnet which is called the inflector is installed along the beam path between the iron wall and the magnet pole region to cancel the fringe field and guide the incoming beam into the storage region of the ring. The length of the inflector is 1.7 m and the aperture for the muon beam in the inflector is 18 mm (width) × 56 mm (height). The storage ring is using weak focusing to store muons. It has 4 electrostatic quadrupoles which are equally spaced around the ring with each extending 39 degree. With quadrupoles operating at ± 32 kV, field index n ($=\frac{R_0}{B_0}\frac{dE}{dR}$) is 0.185, where E is the electric field and R the radial coordinate. As the quads are extended and relatively weak, the closed ring β functions are very nearly constant with $\beta^x_{\mathrm{ring}} = 8$ m, $\beta^y_{\mathrm{ring}} = 16$ m, $\eta^x = 8.5$ m. The horizontal and vertical tunes are 0.903 and 0.440 respectively. To maximize transmission through the narrow aperture of the inflector (18 mm) into the broader aperture of the ring (90 mm) there is necessarily a mismatch. The ratio of the β at the inflector exit (β_{inf}) to peak β in the ring ($\beta_{\mathrm{max\_ring}}$) is chosen so that $\sqrt{\beta^x_{\mathrm{inf}}/\beta^x_{\mathrm{max\_ring}}} = \frac{9\ \mathrm{mm}}{45\ \mathrm{mm}}$, $\sqrt{\beta^y_{\mathrm{inf}}/\beta^y_{\mathrm{max\_ring}}} = \frac{28\ \mathrm{mm}}{45\ \mathrm{mm}}$. Peak β in the ring is given by the relation, $\beta_{\mathrm{max\_ring}} \sim \frac{\beta^2_{\mathrm{ring}}}{\beta_{\mathrm{inf}}}$. Therefore, from these relations, one can find the desirable β_{inf} values as $\beta^x_{\mathrm{inf}} = 1.6$ m, $\beta^y_{\mathrm{inf}} = 10.0$ m. The beam squeezed through the inflector will have α value close to zero midway through the inflector. Another key element in the ring simulation is the kicker. The muon beam coming out of the inflector into the storage region is horizontally 77 mm offset from the center of the storage region and the kicker will provide the transverse kick to steer the beam onto the closed orbit of the ring. The kicker system is located at 90 degree azimuthally downstream from the inflector exit where the incoming beam meets the closed orbit of the ring. The kicker consists of 3 1.27 m long strip line pulsed magnets.

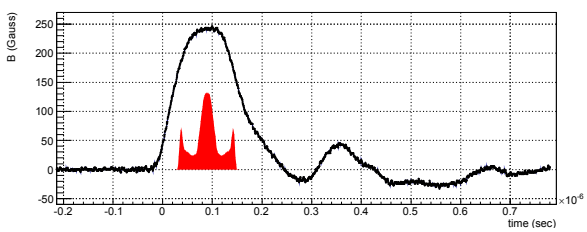

Figure 2: Transient kicker pulse from the prototype kicker. The red histogram represents the incoming muon beam distribution.

Ideally the kicker pulse extends at least the length of the 120 ns long muon bunch and is extinguished in less than the revolution period of 149 ns. The transient kicker pulse from the prototype kicker is seen in Fig. 2. The layout of the storage ring with the key simulation elements are shown in Fig. 3.

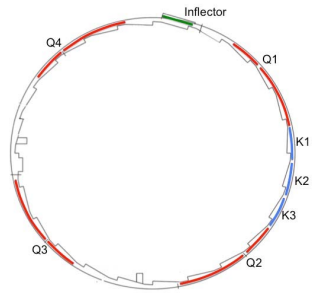

Figure 3: The layout of the storage ring with the inflector, quadrupoles (Q 1-4), kickers (K 1-3).

MUON BEAM INJECTION SIMULATION

We model the injection channel and storage ring kickers and guide fields using the BMAD accelerator library [4]. The injection channel which includes the iron yoke, the fringe field and the inflector is characterized in terms of field maps. The multiple scattering in the superconducting coil which overlaps the entrance and the exit of the inflector are also included . The kicker field map is computed with a finite element code for the design geometry. The kicker pulse in Fig. 2. is adopted for the transient kicker pulse shape in the simulation and the overall strength was scaled for the best muon capture efficiency. The quadrupole fields are implemented by the model of multipole expansion [5]. The muon beam which enters the storage ring will inevitably suffer the multiple scattering with the outer plate of the first quadrupole (Q1) which causes significant muon losses. As it is planned that the outer plate material for Q1 is replaced by a very thin material like an aluminized mylar foil, the multiple scattering in the Q1 outer plate is turned off in the simulation. It is assumed that if a muon hits the inner walls of the inflector or any other aperture which defines the elements, the muon is lost. At first, we tried to find the best beam parameters in the muon storage region which starts from the inflector exit to maximize the muon capture efficiency. Assuming $\alpha = 0$ and $\eta = 0$ at the inflector exit, we varied β value at the inflector exit and propagated the beam parameters backward along the injection channel to the entrance hole on the iron yoke which is the starting point of our muon injection simulation. The muon particles are generated by the corresponding beam parameters at the entrance and propagated forward along the injection channel to the ring and tracked up to 50 revolutions in the ring. For the simplicity of the study, the muon decay was not allowed. We define capture efficiency as the ratio of the number of muons that survive 50 turns to the number incident at the hole in the backleg iron. The results show that the muon capture efficiency reaches the maximum of 4.02% when $\beta_x = 2$ m, $\beta_y = 10$ m (Fig. 4). Given the

scanning step of β, this agrees well with the expectation discussed in the above section. Because there is zero dispersion at the inflector exit, energy acceptance is limited to $\pm$ 0.25 %. The rms energy spread of the beam at the end of M5 line is 1.2 %. Nearly 90 % of the beam that arrives at the ring is outside the energy aperture.

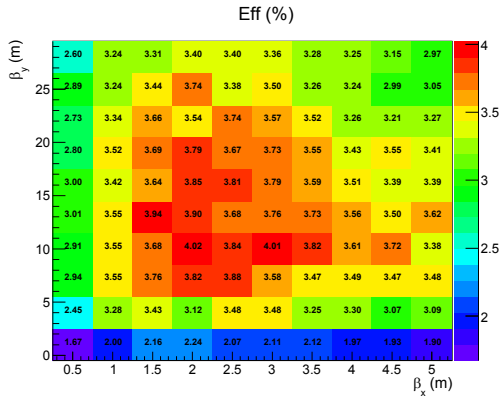

Figure 4: The muon capture efficiency by β at the inflector exit.

With the given $\beta_x = 2$ m, $\beta_y = 10$ m, we tried to fine-tune the α value and found that the capture efficiency is slightly improved when $\alpha_x = -0.4$, $\alpha_y = 0.2$ at the inflector exit. By backward tracking, this beam parameter can be translated as $\beta_{0x} = 33$ m, $\beta_{0y} = 3$ m, $\alpha_{0x} = 10$, $\alpha_{0y} = 3$ where α_0, β_0 are beam parameters at the simulation starting point which is 30 cm before the entrance hole in the iron yoke. For the further step, we include the final focusing quadrupoles of the M5 line located right before the storage ring in the simulation to tune the quadrupoles on the final focusing line so that the muon beam entering the ring has the optimum beam parameters as we found. We inherited the muon distribution right before the final focusing line which was produced by the beamline simulation [3] as the initial distribution and found the corresponding optimal strength of the quadrupoles. After the final focusing line optimization, we found that in the simulation, the muon beam generated in the muon campus beamline ended up in the storage ring with 3.92 % capture efficiency, which is close to about 4 % maximum capture efficiency as estimated above. Recently, we implemented the time-dependent quadrupole field to scrape the muons which are far off the beam center with the collimator in the simulation. By doing the similar study with this new feature and the increased statistics provided by the beamline simulation, we will have more precise estimation.

SPIN TRACKING THROUGH THE INJECTION AND THE RING

We also tracked the spin through the injection and the ring taking the initial spin values from the beamline simulation. The muon beam has a width of 120 ns and since the earlier part of the beam stays longer in the storage ring, the ealier part has a different spin orientation relative to the later part. If the kicker pulse is non-uniform transient pulse, the momentum selection and the energy of the stored beam can vary according to the time when the beam passes by the kicker.

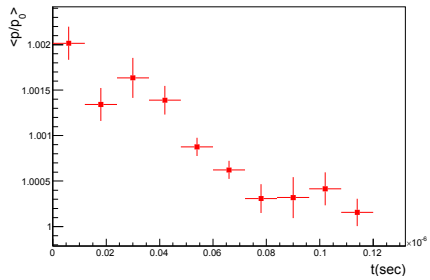

Figure 5: Average momentum (normalized by the magic momentum) as the function of the time when the beam passes by the kicker.

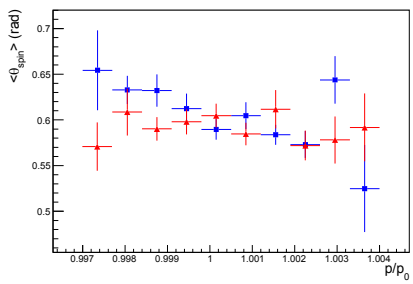

Figure 6: Spin-momentum correlation for the muon beam 200 ns after the injection into the storage ring. The blue one (square) is when the kicker pulse is prototype kicker pulse and the red one (triangle) ideal square kicker pulse.

Assuming the kicker pulse described above, the simulation clearly shows the time dependence of average momentum of the stored beam (Fig. 5). Therefore, the non-uniform kicker pulse can introduce the spin-momentum correlation. Figure 6. Shows the spin-momentum correlation 200 ns after the beam enters the storage ring. In the figure, the case when the kicker pulse is ideal square pulse is also plotted together for the comparison. Even though it is not certain given the lack of enough statistics due to the small capture efficiency, one can see that the case with the prototype kicker shows stronger spin-momentum correlation. We are hoping that the increased statistics from the beamline simulation will help to show more clear picture about the effect of the non-uniform kicker pulse. Our previous work [3] showed that at the end of M5 line, the beam has the spin-momentum correlation. As the muon experiences E-field depending on its momentum in the ring, it will be interesting to see how this spin-momentum correlation develops through many revolutions in the ring.

REFERENCES

[1] J. Grange *et al*., *Muon (g-2) Technical Design Report,* arXiv:1501.06858, 2015.
[2] G. W. Bennett *et al.* [Muon g-2 Collaboration], *Phys. Rev. D* 73, p. 072003, 2006.
[3] D. Stratakis *et al*., in *Proc. IPAC 2016*, paper MOPOY060.
[4] D. Sagan, *Nucl. Instrum. Meth. A*, vol. 558, p. 356, 2006.
[5] Y. K. Semertzidis *et al*., *Nucl. Instrum. Meth. A*, vol. 503, p. 458, 2003.